Supporting Materials

Interleukin-22 ameliorates neutrophil-driven nonalcoholic steatohepatitis through multiple targets

Seonghwan Hwang,[1] Yong He,[1] Xiaogang Xiang,[1] Wonhyo Seo,[1] Seung-Jin Kim,[1] Jing Ma,[1] Tianyi Ren,[1] Seol Hee Park,[1] Zhou Zhou,[1] Dechun Feng,[1] George Kunos,[2] Bin Gao[1]*

[1]Laboratory of Liver Diseases, [2]Laboratory of Physiologic Studies, National Institute on Alcohol Abuse and Alcoholism, National Institutes of Health, Bethesda, MD, 20892, USA

Supplementary Materials and Methods

Liver tissues from NASH patients

Normal and human NASH liver samples (n=5/group) were obtained from the NIH-funded Liver Tissue Cell Distribution System at the University of Minnesota, which was funded by NIH contract # HHSN276201200017C. Information for the characteristics of each patient is included in Supporting Table 1.

MCD-induced NASH model

Male *Ncf1*$^{Lyz-/-}$ and WT littermates or C57BL6/J mice (6-7 weeks of age) were fed an MCD (MP Biomedicals, Solon, OH) for 6 weeks and sacrificed for the collection of serum and liver tissues.

Measurement of serum ALT

Serum ALT levels were determined from the blood drawn from the mouse retro-orbital plexus using Catalyst Dx Chemistry Analyzer (IDEXX Laboratories, Westbrook, ME) according to the manufacturer's instructions.

ELISA analysis

The serum levels of mouse CXCL1 were measured by using Mouse CXCL1/KC Quantikine ELISA kit (R&D Systems, Minneapolis, MN) according to the manufacturer's protocol.

Isolation and culture of mouse primary hepatocytes

For hepatocyte isolation, mice were anesthetized with 30 mg/kg pentobarbital sodium intraperitoneally. Portal vein was cannulated and perfused with ethylene glycol tetraacetic acid and the liver tissue was digested with 0.075% collagenase (Worthington, Lakewood, NJ).[(1)] Primary hepatocytes were collected after centrifugation at 50×g for 5 min and cultured in DMEM containing 10% fetal bovine serum and penicillin-streptomycin. Hepatocytes were pretreated with IL-22Fc (up to 50 ng/mL) for 20 hr, followed by treatment with H_2O_2 (1.5 mM) for 30 min and subjected to immunoblot analysis of phosphorylated stress kinases, or treatment with H_2O_2 (0.5 mM) for 5 hr and subjected to immunoblot analysis of caspase 3 and MT protein expression.

Isolation of mouse bone marrow-derived neutrophils

Mouse bone marrow was collected from femur and tibia and passed through a 70 μm cell strainer in PBS, and the cell suspension was centrifuged at 300×g for 5 min. The resulting leukocyte pellet was resuspended in ACK lysing buffer (BioWhittaker, Walkersville, MD). After incubation for 2 min on ice, the cells were washed in PBS. The leukocytes were subjected to neutrophil isolation by using Neutrophil Isolation Kit (Miltenyi Biotec, San Diego, CA) according to the manufacturer's instructions.

Coculture of neutrophils with AML12 cells and chemotaxis assay

Mouse hepatocyte cell line AML12 cells were cultured in a 1:1 mixture of DMEM and Ham's F12 medium with 0.005 mg/mL insulin, 0.005 mg/mL transferrin, 5 ng/mL selenium, 40 ng/mL dexamethasone, 10% fetal bovine serum, and penicillin-streptomycin. For chemotaxis assay, AML12 cells were cultured in the bottom chamber of 6-well cell culture plate until cells reached 80% confluence, and neutrophils (1×10^6 cells) isolated from mouse bone marrow were added onto the insert (3 μm pore size) in RPMI1640 media supplemented with 10% fetal bovine serum and penicillin-streptomycin. AML12 cells were further treated with a recombinant mouse CXCL1 protein or DPI (Sigma, St. Louis, MO). Migrating neutrophils were collected from the bottom

chamber media and subjected to hemocytometer-assisted cell counting after low-speed centrifugation to remove AML12 cells.

Flow cytometry analysis of ROS

ROS levels in AML12 cells and primary mouse hepatocytes were measured using DCFDA Cellular ROS Detection Assay Kit (Abcam, Cambridge, MA) according to the manufacturer's manual with minor modifications. Briefly, after incubation with IL-22Fc (50 ng/mL) and/or H_2O_2, cells were harvested with trypsinization and further incubated in 5 μM DCFDA at 37ºC for 30 min. DCF intensity was measured by flow cytometry in FL1 channel (CytoFLEX, Beckman Coulter, Brea, CA). The concentrations of H_2O_2 for AML12 cells and primary mouse hepatocytes were 0.125 mM and 0.25 mM, respectively.

Flow cytometry analysis of hepatic neutrophil infiltration

Liver tissues were passed through a 70 μm cell strainer in PBS, and the cell suspension was centrifuged at 30×g for 5 min to pellet hepatocytes. The supernatant, which was enriched in non-parenchymal cells, was centrifuged at 300×g for 10 min. The pellet was resuspended in 10 mL of 40% Percoll (GE Healthcare, Pittsburgh, PA) and centrifuged at 500×g for 15 min. The resulting leukocyte pellet was resuspended in 2 mL of ACK lysing buffer (BioWhittaker, Walkersville, MD). After incubation for 2 min on ice, the cells were washed in PBS. Dead cells were stained with Zombie Yellow Kit (BioLegend, San Diego, CA). Single-cell suspension was incubated with antibodies against CD45 (Thermo Fisher-eBioscience, Waltham, MA), CD11b (Thermo Fisher-eBioscience, Waltham, MA), and Ly6G (Thermo Fisher-eBioscience, Waltham, MA). Flow cytometry data were obtained from CytoFLEX (Beckman Coulter, Brea, CA) and analyzed by FlowJo software (BD, San Jose, CA).

Isolation of neutrophils, monocytes, Kupffer cells, and dendritic cells by flow cytometry cell sorting

For isolation of neutrophils and monocytes, mouse bone marrow was collected from femur and tibia and passed through a 70 μm cell strainer in PBS, and the cell suspension was centrifuged at 300×g for 5 min. The resulting leukocyte pellet was resuspended in ACK lysing buffer (BioWhittaker, Walkersville, MD). After incubation for 2 min on ice, the cells were washed in

PBS. Single-cell suspension of the leukocytes was incubated with Zombie Violet Kit (BioLegend, San Diego, CA) to exclude dead cells and stained with antibodies against CD45, CD11b, CD115, Ly6G (Thermo Fisher-eBioscience, Waltham, MA), and CCR2 (BioLegend, San Diego, CA).

For isolation of Kupffer cells, portal vein was cannulated and perfused with ethylene glycol tetraacetic acid and the liver tissue was digested with 0.075% collagenase (Worthington, Lakewood, NJ). The cell suspension was centrifuged at 30×g for 5 min to pellet hepatocytes. The supernatant was centrifuged at 460×g for 10 min. The pellet was resuspended in 35% Percoll (GE Healthcare, Pittsburgh, PA) and centrifuged at 450×g for 15 min. The pellet was incubated with ACK lysing buffer (BioWhittaker, Walkersville, MD). After incubation for 2 min on ice, the cells were washed in PBS. Single-cell suspension was incubated with antibodies against CD45, CD11b, F4/80, and Ly6G (Thermo Fisher-eBioscience, Waltham, MA).

For isolation of dendritic cells, spleen was passed through a 70 μm cell strainer in PBS, and the cell suspension was centrifuged at 300×g for 5 min. The resulting leukocyte pellet was resuspended in ACK lysing buffer (BioWhittaker, Walkersville, MD). After incubation for 2 min on ice, the cells were subjected to enrichment of $CD11c^+$ cells using CD11c MicroBeads (Miltenyi Biotec, San Diego, CA). The resultant CD11c-enriched cells were subjected to staining with Zombie Violet (BioLegend, San Diego, CA) to exclude dead cells and stained with antibodies against CD45, CD11c, and MHCII (Thermo Fisher-eBioscience, Waltham, MA).

Cell sorting was performed by FACSMelody (BD, San Jose, CA) according to the manufacturer's instructions. $CD45^+$ $CD11b^+$ $CD115^+$ $CCR2^+$ cell population was defined as monocytes, $CD45^+$ $CD11b^+$ $Ly6G^+$ cell population was defined as neutrophils, $CD45^+$ $CD11b^{lo}$ $F4/80^{hi}$ $Ly6G^-$ cell population was defined as Kupffer cells, and $CD45^+$ $CD11c^+$ $MHCII^+$ cells population was defined as dendritic cells.

Histological and immunohistochemical analysis

Formalin-fixed liver samples were processed, and 4-μm-thick paraffin sections were stained with Sirius Red dyes (Sigma, St. Louis, MO). TUNEL staining was performed with an ApopTag® Peroxidase *In Situ* Apoptosis Detection Kit (Millipore, Burlington, MA). For immunohistochemistry, after heat-induced epitope retrieval, paraffin-embedded sections were incubated in 3% H_2O_2 and blocked in 3% normal serum buffer. Sections were incubated with

primary antibodies overnight at 4°C. Vectastain Elite ABC Staining Kit and DAB Peroxidase Substrate Kit (Vector Laboratories, Burlingame, CA) were used to visualize the staining according to the manufacturer's instructions. Primary antibodies used include those specific to MPO (Biocare Medical, Concord, CA), Ly6G (BioXCell, West Lebanon, NH), MDA (Genox, Baltimore, MD), 4-HNE (Genox, Baltimore, MD), F4/80 (Cell Signaling Technology, Danvers, MA), CXCL1 (R&D Systems, Minneapolis, MN), and α-SMA (Agilent DAKO, Santa Clara, CA). Positive cells and positive areas in 10 randomly selected high-power fields were analyzed.

Immunoblot analysis

Liver tissues and cells were homogenized or lysed in RIPA buffer containing a cocktail of protease inhibitors (Santa Cruz Biotechnology, Dallas, TX) according to the manufacturer's instructions. Protein extracts were loaded onto 4-12% Bis-Tris protein gels (Bio-Rad, Hercules, CA) and transferred onto nitrocellulose membranes (Thermo Fisher, Waltham, MA). Protein bands were visualized with Pierce ECL Western Blotting Substrate (Thermo Fisher, Waltham, MA). The antibodies against cleaved CASP3, CASP3, p-p38 (Thr180/Tyr182), p38, p-JNK (Thr183/Tyr185), JNK, p-STAT3 (Tyr705), and STAT3 were purchased from Cell Signaling Technology (Danvers, MA). The antibodies against p-ASK1 (Thr838) and ASK1 were purchased from Thermo Fisher (Waltham, MA). The antibodies against MT and β-actin were purchased from Abcam (Cambridge, MA). The antibody against CD63 was purchased from Santa Cruz Biotechnology. The antibody against ALIX was purchased from System Biosciences (Palo Alto, CA).

Total RNA isolation and RT-qPCR

Total RNA was purified from liver tissues or cell cultures using TRIzol reagents (Thermo Fisher, Waltham, MA) according to the manufacturer's instructions. One microgram of RNA was reverse-transcribed into cDNA using a High-Capacity cDNA Reverse Transcription Kit (Thermo Fisher, Waltham, MA). The expression levels of mRNA were measured by RT-qPCR with an ABI7500 RT-PCR system (Applied Biosystems, Foster City, CA). *Gapdh* or *Apob* was used as the invariant control. The $2^{-\Delta\Delta Ct}$ method was used to calculate the level of mRNA. The primer sequences used for PCR reactions are listed in Supporting Table 2.

Measurement of cell death by trypan blue assay

The percentage of dead cells was determined by trypan blue assay as previously described.[2] Briefly, primary hepatocytes were treated with H_2O_2 or TNF-α preceded by pretreatment with IL-22Fc (Generon, Corporation, Shanghai, China), LY2228820, or PH797804 (Selleckchem, Houston, TX) as indicated in Figure Legends and harvested using Trypsin-EDTA. After a low-speed centrifugation, the cell pellet was resuspended in 1 mL PBS, 50 μL of which was mixed with the same volume of trypan blue (0.4%) and subjected to hemocytometer-assisted cell counting.

EV isolation and cell treatment

EVs were isolated as previously described.[3, 4] Briefly, after centrifugation of blood serum or culture medium at 3,000×g for 15 min at 4°C, the supernatant fraction including EVs was incubated with an appropriate volume of ExoQuick or ExoQuick-TC exosome precipitation solution (System Biosciences, Palo Alto, CA) depending on the type of samples and subjected to EV isolation procedure according to the manufacturer's manual. The size of EVs was assessed using Nanosight NS300 System (Malvern Instruments, Malvern, UK) equipped with a fast video capture and nanoparticle tracking analysis, and the concentration of EVs was measured by using the Pierce BCA protein assay kit (Thermo Fisher, Waltham, MA) and EXOCET Exosome Quantitation Kit (System Biosciences, Palo Alto, CA).

RAW264.7 cells were cultured in RPMI1640 media supplemented with 10% fetal bovine serum and penicillin-streptomycin. At 80% confluence, cells were starved of serum for 3 hr and treated with EVs (5 μg/mL) for 3 hr. For inhibition of TLR9, RAW264.7 cells were pretreated with 2 μM of ODN2088 or control (InvivoGen, San Diego, CA) for 1 hr.

Quantification of mtDNA in EVs

After quantification of EVs using BCA protein assay, an equal amount of EVs was subjected to DNA extraction using QIAmp DNA Mini kit (Qiagen, Germantown, MD) as previously described.[3, 4] Extracted DNA was further quantified using NanoDrop™ spectrometer (Thermo Fisher, Waltham, MA) and an equal amount of DNA was subjected to real-time PCR reaction using the primers for the mitochondrial genome-specific genes (e.g., *Atp6, Cox3, and Nd2*). The primer sequences used for PCR reactions are listed in Supporting Table 2.

References

1) He Y, Hwang S, Cai Y, Kim SJ, Xu M, Yang D, et al. MicroRNA-223 Ameliorates Nonalcoholic Steatohepatitis and Cancer by Targeting Multiple Inflammatory and Oncogenic Genes in Hepatocytes. Hepatology 2019;70:1150-1167.
2) Crowley LC, Marfell BJ, Christensen ME, Waterhouse NJ. Measuring Cell Death by Trypan Blue Uptake and Light Microscopy. Cold Spring Harb Protoc 2016.
3) **Cai Y**, **Xu MJ**, Koritzinsky EH, Zhou Z, Wang W, Cao H, et al. Mitochondrial DNA-enriched microparticles promote acute-on-chronic alcoholic neutrophilia and hepatotoxicity. JCI Insight 2017;2:e92634.
4) **Seo W**, **Gao Y**, He Y, Sun J, Xu H, Feng D, et al. ALDH2 deficiency promotes alcohol-associated liver cancer by activating oncogenic pathways via oxidized DNA enriched extracellular vesicles. J Hepatol 2019;71:1000-1011.

Author names in bold designate shared co-first authorship.

Supporting Table 1. General characteristics of the NASH human liver samples

#	Gender	Age	Primary Diagnosis
1	F	60	end-stage liver disease secondary to NASH; cirrhosis
2	F	62	end-stage liver disease; fatty liver; cirrhosis
3	M	56	end-stage liver disease secondary to NASH; diabetes for 10 years
4	F	59	cirrhosis secondary to NASH
5	F	61	NASH with end-stage liver disease; cirrhosis; morbidly obese

Supporting Table 2. Primer sequences for real time PCR

Gene Name	Forward (5'-3')	Reverse (5'-3')
Acta2	TCCTGACGCTGAAGTATCCGATA	GGTGCCAGATCTTTTCCATGTC
Adgre5	ATTCCACCGTCTGCAAAAACA	GGGCAGCAGTGTCCAAGTAG
Anxa1	ATGTATCCTCGGATGTTGCTGC	TGAGCATTGGTCCTCTTGGTA
Apob	CGTGGGCTCCAGCATTCTA	TCACCAGTCATTTCTGCCTTTG
Atp6	GCTCTCACTCGCCCACTTCCTTCC	GCCGGACTGCTAATGCCATTGGTT
Ccl19	GGGGTGCTAATGATGCGGAA	CCTTAGTGTGGTGAACACAACA
Ccl2	TCTGGACCCATTCCTTCTTGG	TCAGCCAGATGCAGTTAACGC
Ccl20	GCCTCTCGTACATACAGACGC	CCAGTTCTGCTTTGGATCAGC
Ccl21	GTGATGGAGGGGGTCAGGA	GGGATGGGACAGCCTAAACT
Ccl5	GCTGCTTTGCCTACCTCTCC	TCGAGTGACAAACACGACTGC
Cd40lg	CCTTGCTGAACTGTGAGGAGA	CTTCGCTTACAACGTGTGCT
Col12a1	AAGTTGACCCACCTTCCGAC	GGTCCACTGTTATTCTGTAACCC
Col15a1	CCCAGGGAAGAATGGAGAAGT	CCAGAGCCTTCAATCTCAAATCC
Col1a1	TAGGCCATTGTGTATGCAGC	ACATGTTCAGCTTTGTGGACC
Col1a2	GGTGAGCCTGGTCAAACGG	ACTGTGTCCTTTCACGCCTTT
Col3a1	TAGGACTGACCAAGGTGGCT	GGAACCTGGTTTCTTCTCACC
Col4a1	CACATTTTCCACAGCCAGAG	GTCTGGCTTCTGCTGCTCTT
Col4a2	GACCGAGTGCGGTTCAAAG	CGCAGGGCACATCCAACTT
Col5a2	TTGGAAACCTTCTCCATGTCAGA	TCCCCAGTGGGTGTTATAGGA
Col6a3	GCTGCGGAATCACTTTGTGC	CACCTTGACACCTTTCTGGGT
Cox3	ACCAAGGCCACCACACTCCT	ACGCTCAGAAGAATCCTGCAAAGAA
Ctgf	GGGCCTCTTCTGCGATTTC	ATCCAGGCAAGTGCATTGGTA
Ctsk	GAAGAAGACTCACCAGAAGCAG	TCCAGGTTATGGGCAGAGATT
Cxcl1	ACTGCACCCAAACCGAAGTC	TGGGGACACCTTTTAGCATCTT
Cxcl10	CCAAGCCTTATCGGAAATGA	TTTTCACAGGGGAGAAATCG

Cxcl12	TGCATCAGTGACGGTAAACCA	TTCTTCAGCCGTGCAACAATC
Cxcr4	GAAGTGGGGTCTGGAGACTAT	TTGCCGACTATGCCAGTCAAG
Ereg	CTGCCTCTTGGGTCTTGACG	GCGGTACAGTTATCCTCGGATTC
F4/80	CTTTGGCTATGGGCTTCCAGTC	GCAAGGAGGACAGAGTTTATCGTG
Fos	CGGGTTTCAACGCCGACTA	TTGGCACTAGAGACGGACAGA
Fosl2	CCAGCAGAAGTTCCGGGTAG	GTAGGGATGTGAGCGTGGATA
Gapdh	AGCAGCCGCATCTTCTTGTGCAGTG	GGCCTTGACTGTGCCGTTGAATTT
gp91phox (Nox2)	GACCATTGCAAGTGAACACCC	AAATGAAGTGGACTCCACGCG
Il18	GACTCTTGCGTCAACTTCAAGG	CAGGCTGTCTTTTGTCAACGA
Il1b	TCGCTCAGGGTCACAAGAAA	CATCAGAGGCAAGGAGGAAAAC
Il2rg	CTCAGGCAACCAACCTCAC	GCTGGACAACAAATGTCTGGTAG
Il6	ACAAGTCGGAGGCTTAATTACACAT	TTGCCATTGCACAACTCTTTTC
Il7r	GCGGACGATCACTCCTTCTG	AGCCCCACATATTTGAAATTCCA
Jun	CCTTCTACGACGATGCCCTC	GGTTCAAGGTCATGCTCTGTTT
Ly6g	TGCGTTGCTCTGGAGATAGA	CAGAGTAGTGGGGCAGATGG
Lyz1	GAGACCGAAGCACCGACTATG	CGGTTTTGACATTGTGTTCGC
Mmp14	CAGTATGGCTACCTACCTCCAG	GCCTTGCCTGTCACTTGTAAA
Mmp19	GCTGACATTCGCCTCTCTTTC	CACTCCTTGATAGGTCCCCTC
Mmp2	CAAGTTCCCCGGCGATGTC	TTCTGGTCAAGGTCACCTGTC
Mmp7	CTGCCACTGTCCCAGGAAG	GGGAGAGTTTTCCAGTCATGG
Mt1	AAGAGTGAGTTGGGACACCTT	CGAGACAATACAATGGCCTCC
Mt2	GCCTGCAAATGCAAACAATGC	AGCTGCACTTGTCGGAAGC
Nd2	TCCTCCTGGCCATCGTACTCAACT	AGAAGTGGAATGGGGCGAGGC
p22phox	ATGGAGCGATGTGGACAGAAG	TAGATCACACTGGCAATGGCC
p40phox (Ncf4)	ATCGTCTGGAAGCTGCTCAA	CCCATCCATCTGCTTTTCTG
p47phox (Ncf1)	TCCTCTTCAACAGCAGCGTA	CTATCTGGAGCCCCTTGACA
p67phox (Ncf2)	TCTATCAGCTGGTTCCCACG	TGGCCTACTTCCAGAGAGGA
Pdgfa	GAGGAAGCCGAGATACCCC	TGCTGTGGATCTGACTTCGAG
Pdgfd	TACAGTTGCACTCCCAGGAAT	CTTCCAGTTGACAGTTCCGCA
Pdgfra	TCCATGCTAGACTCAGAAGTCA	TCCCGGTGGACACAATTTTTC
Pdgfrb	TTCCAGGAGTGATACCAGCTT	AGGGGGCGTGATGACTAGG
Rel	AGAGGGGAATGCGGTTTAGAT	TTCTGGTCCAAATTCTGCTTCAT
Sele	AGCAGAGTTTCACGTTGCAGG	TGGCGCAGATAAGGCTTCA
Tgfb1	CAACCCAGGTCCTTCCTAAA	GGAGAGCCCTGGATACCAAC
Tgfb2	CTTCGACGTGACAGACGCT	GCAGGGGCAGTGTAAACTTATT
Tnfa	AGGCTGCCCCGACTACGT	GACTTTCTCCTGGTATGAGATAGCAAA

Tnfaip3	GAACAGCGATCAGGCCAGG	GGACAGTTGGGTGTCTCACATT
Tnfrsf11b	ACCCAGAAACTGGTCATCAGC	CTGCAATACACACACTCATCACT
Tnfrsf21	GCCATGTTGACCGTACCACT	CAGACTCGCAGGCTCATGTT
Vcam1	TGAACCCAAACAGAGGCAGAGT	GGTATCCCATCACTTGAGCAGG

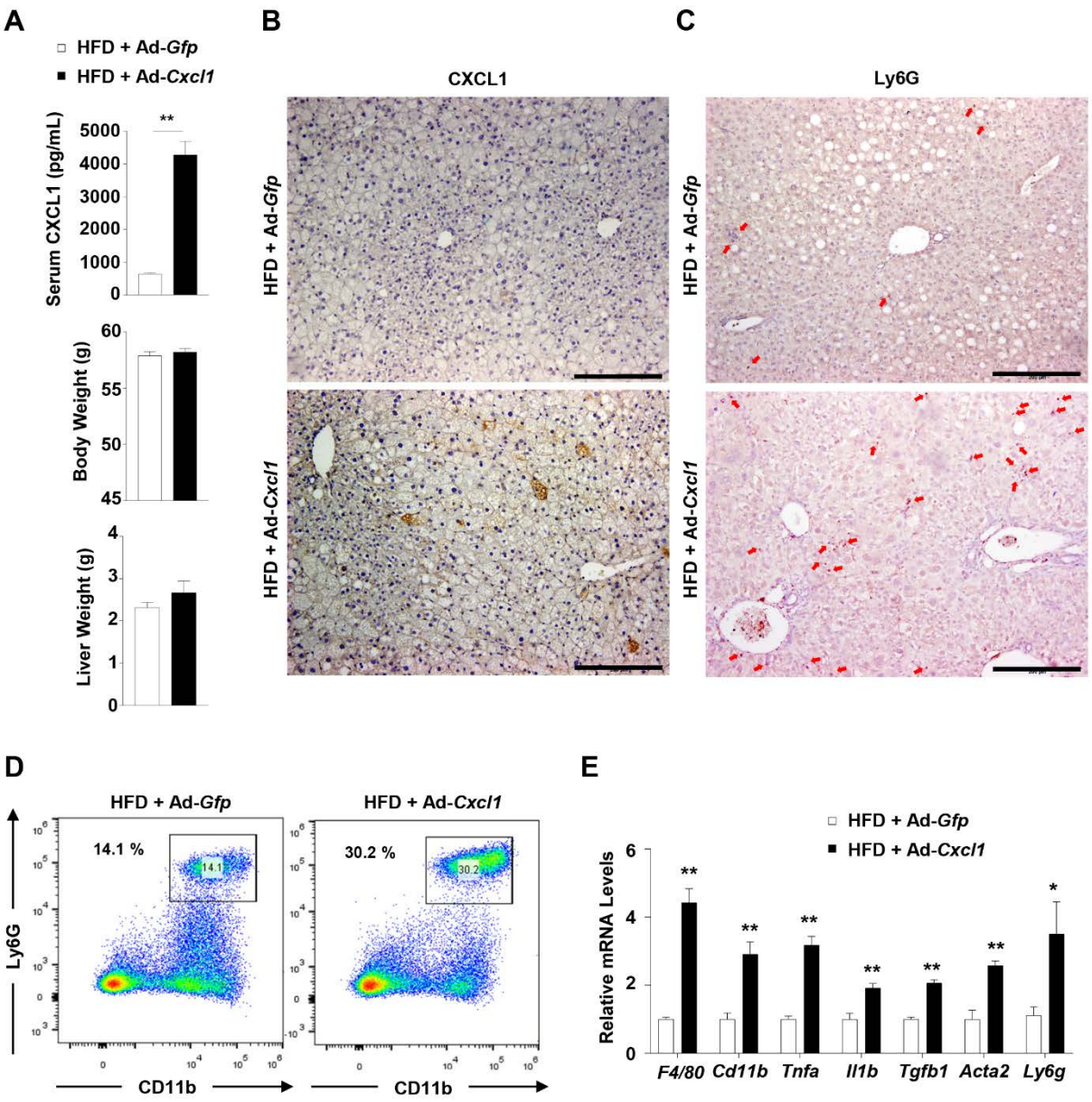

Supporting Fig. S1. Hepatic CXCL1 overexpression in HFD-fed mice promotes neutrophil infiltration in the liver. (A) C57BL/6 mice fed an HFD for 3 months were infected with Ad-*Gfp* or Ad-*Cxcl1* and were sacrificed at 2 weeks after infection (n=6/group). Serum CXCL1 levels, body weight, and liver weight (panel A). Immunohistochemical analysis of CXCL1 in the liver (panel B). Immunohistochemical analysis of Ly6G in the liver. Red arrows indicate Ly6G-positive neutrophils (panel C). Flow cytometry analysis of $CD45^{+}CD11b^{+}Ly6G^{+}$ neutrophil population from liver mononuclear cells (panel D). Hepatic expression of inflammatory genes, fibrogenic genes, and *Ly6g* (a neutrophil marker) was determined by RT-qPCR analysis (n=6/group) (panel E). Scale bars indicate 200 μm. Values represent mean ± SEM. Statistical evaluation was performed by Student's t-test (*p<0.05; **p<0.01).

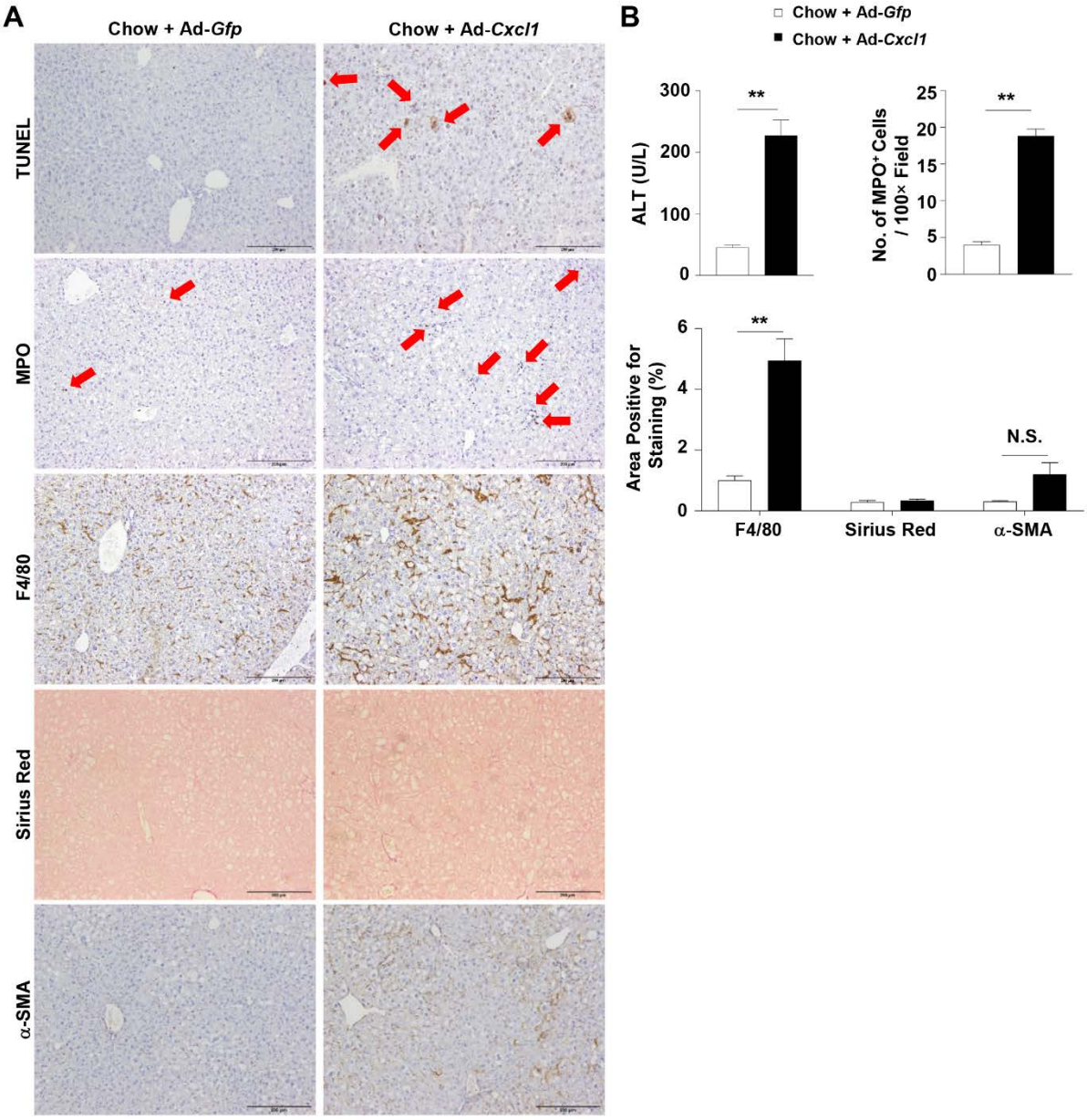

Supporting Fig. S2. Hepatic CXCL1 overexpression in chow-fed mice promotes hepatocyte death, neutrophil infiltration, and inflammation without steatosis and fibrosis. (A) Chow-fed C57BL/6 mice were infected with Ad-*Gfp* or Ad-*Cxcl1,* and paraffin-embedded liver sections prepared at 2 weeks after the infection were subjected to various stainings (n=4/group). Red arrows indicate the TUNEL-positive hepatocytes (TUNEL images) or clusters of MPO-positive neutrophils (MPO images). Scale bars indicate 200 μm. (B) Serum ALT levels and quantification of MPO, F4/80, Sirius Red, and α-SMA staining. Values represent mean ± SEM. Statistical evaluation was performed by Student's t-test (**p<0.01). N.S., not significant.

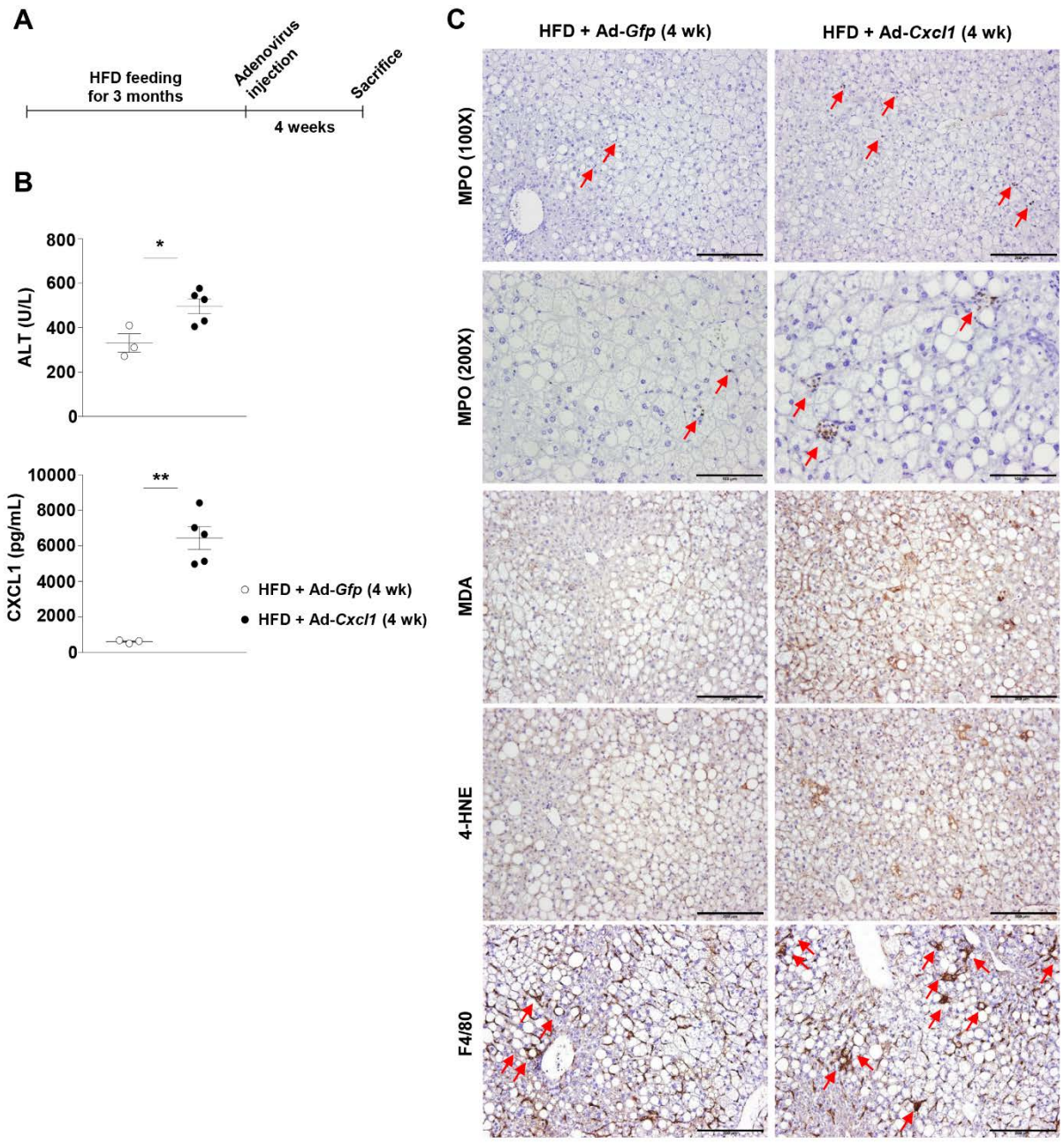

Supporting Fig. S3A-C. The NASH-inducing effect of Ad-*Cxcl1* in HFD-fed mice is observed 4 weeks post infection. (A-C) HFD-fed C57BL/6 mice were infected with Ad-*Gfp* or Ad-*Cxcl1,* and sacrificed for analysis at 4 weeks after infection. A schematic illustration of the experimental design (panel A). Serum ALT and CXCL1 levels (panel B). Paraffin-embedded liver sections were subjected to various stainings (n=3-5/group) (panel C). Red arrows indicate MPO-positive cells (MPO images) or hepatic crown-like structures (F4/80 images). Scale bars indicate 200 μm for every image except for 200X MPO staining images (100 μm). Values represent mean ± SEM. Statistical evaluation was performed by Student's t-test (*p<0.05; **p<0.01).

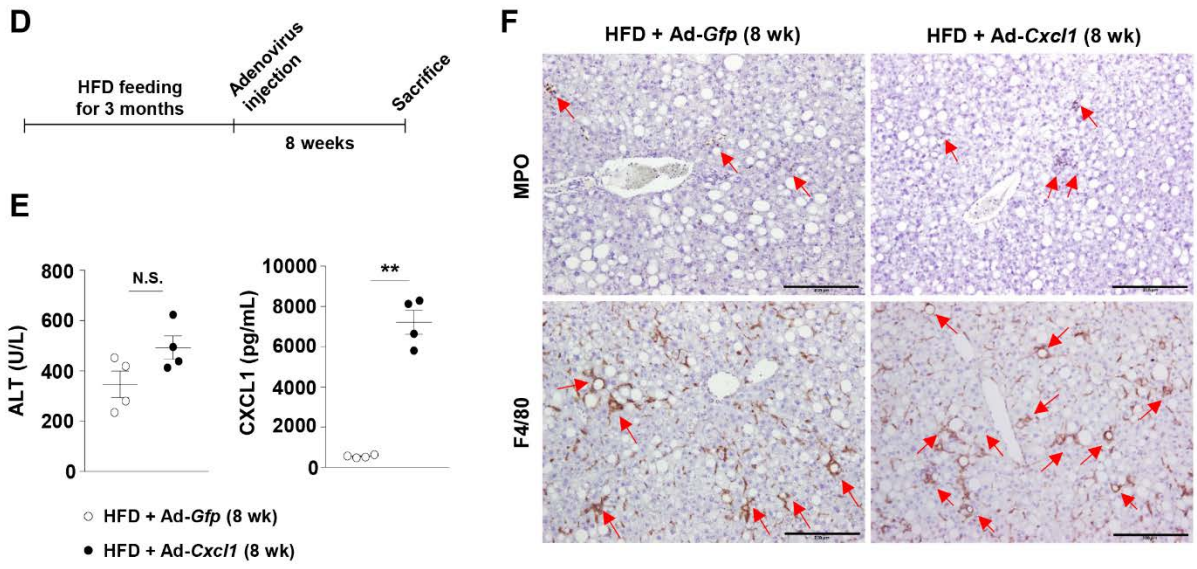

Supporting Fig. S3D-F. The NASH-inducing effect of Ad-*Cxcl1* in HFD-fed mice remains up to 8 weeks post infection. (D-F) HFD-fed C57BL/6 mice were infected with Ad-*Gfp* or Ad-*Cxcl1* and sacrificed for analysis at 8 weeks after infection. A schematic illustration of the experimental design (panel D). Serum ALT and CXCL1 levels (panel E). Paraffin-embedded liver sections were subjected to MPO and F4/80 stainings (n=4/group) (panel F). Red arrows indicate MPO-positive cells (MPO images) or hepatic crown-like structures (F4/80 images). Scale bars indicate 200 μm. Values represent mean ± SEM. Statistical evaluation was performed by Student's t-test (**p<0.01). N.S., not significant.

A

Term	Gene Count	%	P-Value	Benjamini
1. Cell Adhesion	85	9.2	1.9×10^{-26}	6.5×10^{-23}
2. Extracellular Matrix Organization	51	5.5	1.1×10^{-22}	1.9×10^{-19}
3. Cell Chemotaxis	20	2.2	1.5×10^{-10}	1.4×10^{-7}
4. Immune Response	49	5.3	4.5×10^{-8}	1.6×10^{-5}
5. Collagen Fibril Organization	13	1.4	2.0×10^{-7}	6.5×10^{-5}
6. Wound Healing	17	1.8	1.4×10^{-6}	3.4×10^{-4}
7. Inflammatory Response	41	4.5	4.2×10^{-6}	9.3×10^{-4}
8. Positive Regulation of Fibroblast Proliferation	12	1.3	5.1×10^{-6}	4.6×10^{-3}
9. Collagen Catabolic Process	14	1.5	1.1×10^{-5}	1.5×10^{-3}

B

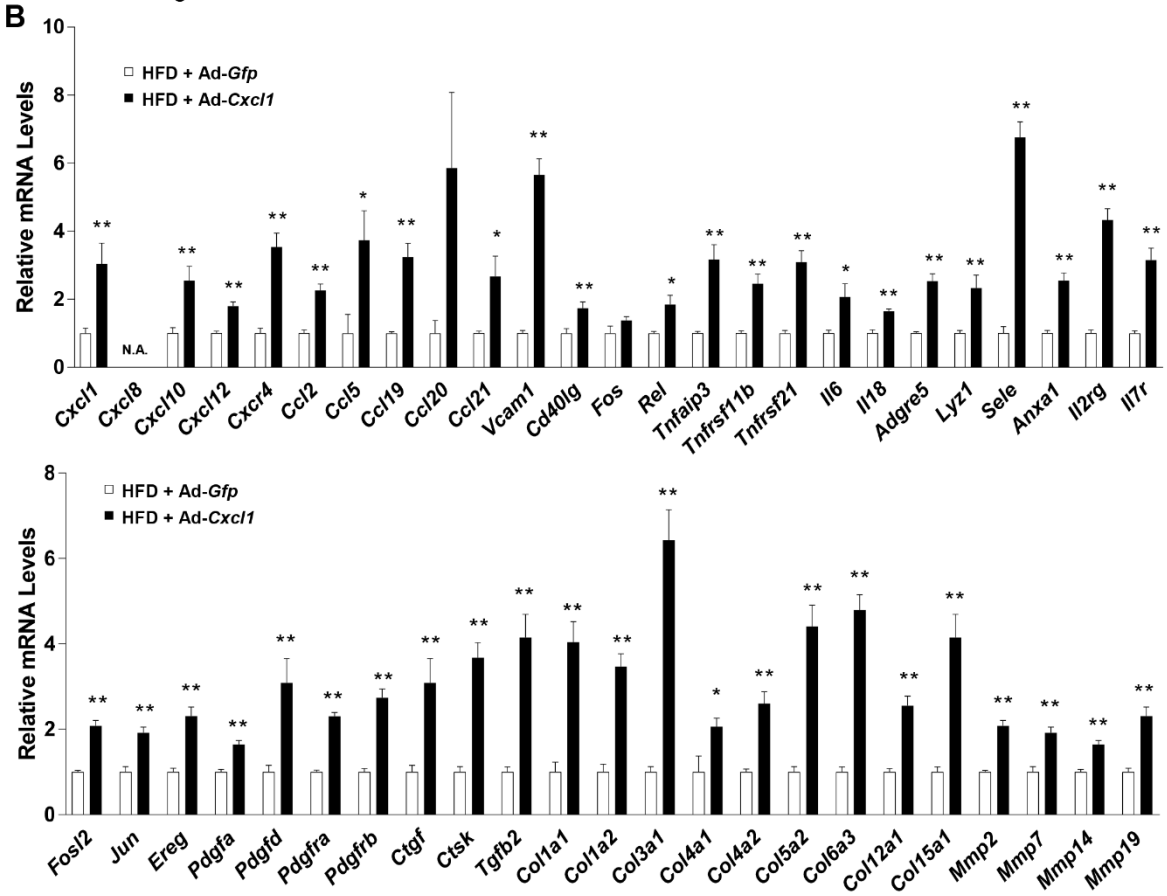

Supporting Fig. S4. CXCL1 overexpression in HFD-fed mice upregulates inflammatory and fibrogenic genes similarly to the gene expression patterns of human NASH patients. (A) Genes upregulated in human NASH by greater than 1.5-fold compared with steatosis were identified from a published microarray data (Lake et al., *Drug Metab Dispos* 2011, 39:1954-1960) and were subjected to DAVID Gene Functional Classification Tool for Gene Enrichment and Functional Annotation analysis. Gene functions associated with the pathogenesis of NASH were demonstrated to be highly enriched in NASH patients. (B) Liver homogenates of HFD-fed mice infected with Ad-*Gfp* or Ad-*Cxcl1* (n=6/group) were subjected to RT-qPCR analysis of the mouse homologs of the 47 human genes upregulated in NASH patients. Values represent mean ± SEM. Statistical evaluation was performed by Student's t-test (**p*<0.05; ***p*<0.01). N.A., not available.

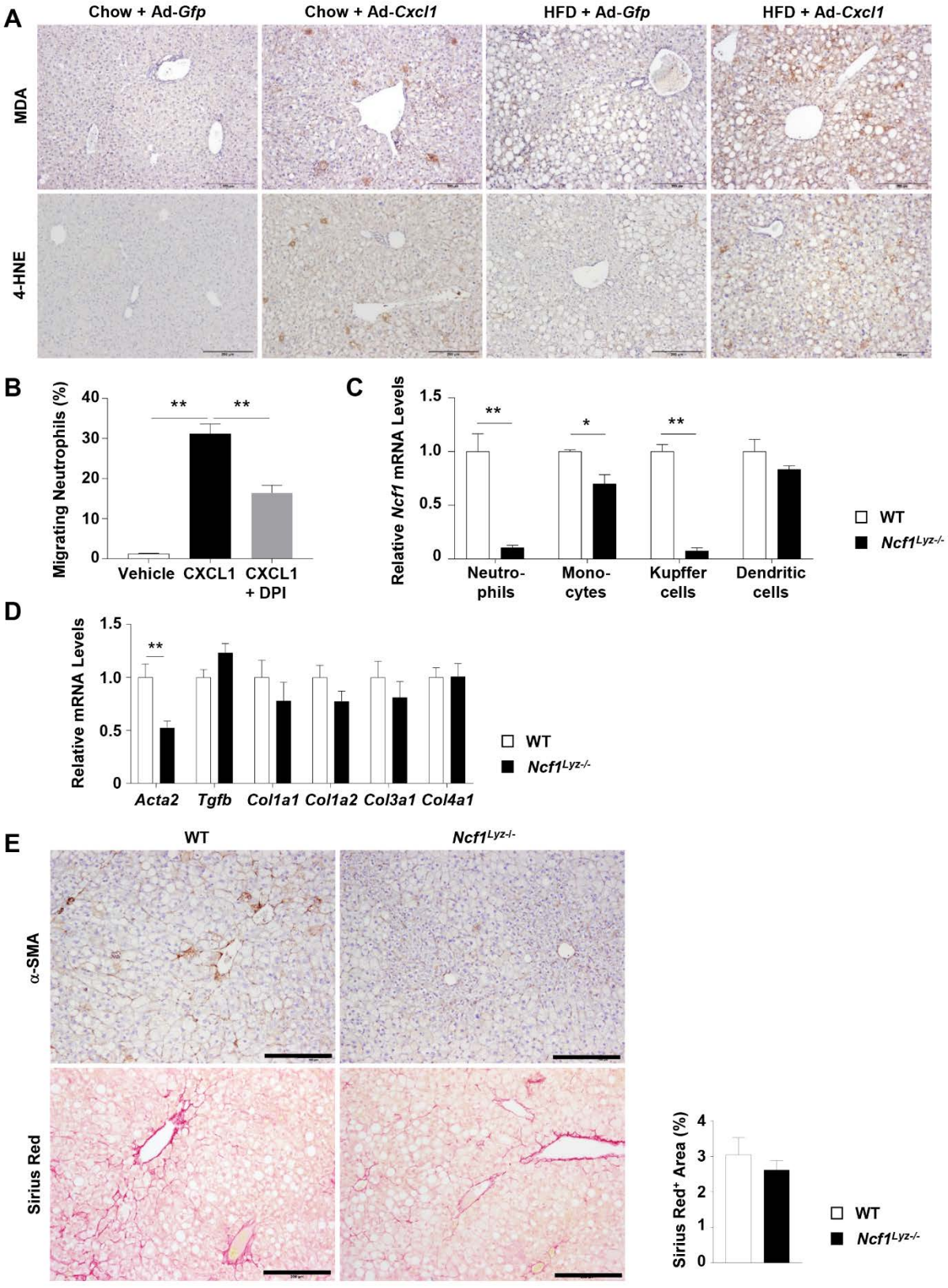
A
Chow + Ad-Gfp
Chow + Ad-Cxcl1
HFD + Ad-Gfp
HFD + Ad-Cxcl1
MDA
4-HNE
B
Migrating Neutrophils (%)
40
30
20
10
0
**
**
Vehicle
CXCL1
CXCL1 + DPI
C
Relative Ncf1 mRNA Levels
1.5
1.0
0.5
0
**
*
**
Neutro-phils
Mono-cytes
Kupffer cells
Dendritic cells
WT
Ncf1Lyz-/-
D
Relative mRNA Levels
1.5
1.0
0.5
0
**
Acta2
Tgfb
Col1a1
Col1a2
Col3a1
Col4a1
WT
Ncf1Lyz-/-
E
WT
Ncf1Lyz-/-
α-SMA
Sirius Red
Sirius Red+ Area (%)
4
3
2
1
0
WT
Ncf1Lyz-/-

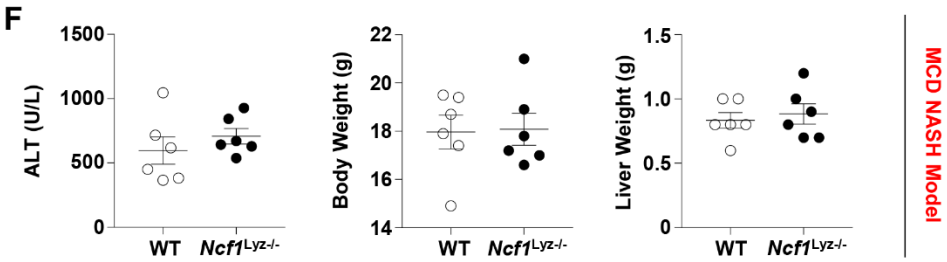

Supporting Fig. S5. (A-E) CXCL1-induced NASH development in mice involves enhanced oxidative stress which is dependent on NCF1-induced neutrophil oxidative burst. (A) HFD- or chow-fed C57BL/6J mice were infected with Ad-*Gfp* or Ad-*Cxcl1* for 2 weeks. Immunohistochemistry of MDA and 4-HNE in the liver sections. (B) Neutrophils (1×10^6 cells) were placed onto the insert (3 μm pore size) of transwell system, and a recombinant mouse CXCL1 protein (100 ng/mL) was added to the bottom chamber (6 hr) where AML12 cells were cultured. DPI (5 μM) was added to the bottom chamber at 30 min prior to CXCL1 treatment. The percentage of the migrating neutrophils to lower chamber relative to total neutrophils added onto the insert (1×10^6 cells) was measured (n=3). (C) mRNA levels of *Ncf1* were measured from neutrophils (bone marrow), monocytes (bone marrow), Kupffer cells, and dendritic cells (spleen) obtained from WT and *Ncf1*$^{Lyz-/-}$ mice by FACS sorting. Results indicate the mean of triplicates. (D, E) WT and *Ncf1*$^{Lyz-/-}$ mice were subjected to HFD+Ad-*Cxcl1* treatment. Liver tissues were subjected to RT-qPCR analysis of fibrogenic genes (n=6/group) in panel D. Paraffin-embedded liver sections of WT and *Ncf1*$^{Lyz-/-}$ mice were subjected to α-SMA and Sirius Red stainings in panel E. Scale bars indicate 200 μm. Values represent mean ± SEM. Statistical evaluation was performed by Student's t-test or one-way ANOVA followed by Tukey's post hoc test for multiple comparisons (**p<0.01). **(F) NCF1/p47^{phox} does not contribute to liver injury in MCD-induced NASH.** WT and *Ncf1*$^{Lyz-/-}$ mice were fed an MCD for 6 weeks. Serum ALT levels, body weight, and liver weight were measured.

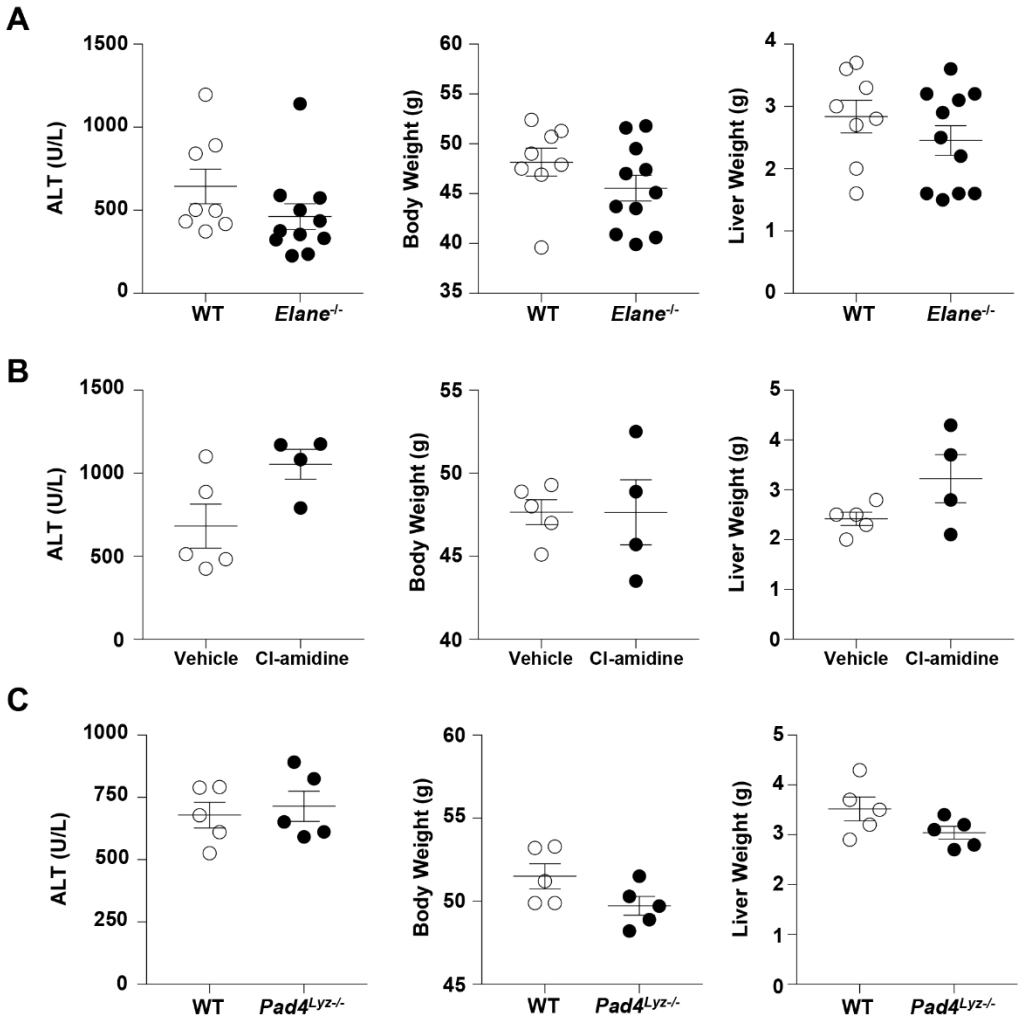

Supporting Fig. S6. Neutrophil elastase or NET formation is not involved in CXCL1-induced NASH development in mice. (A) HFD-fed *Elane*$^{-/-}$ and WT littermate control mice were subjected to a 2-week infection with Ad-*Cxcl1*. *Elane*$^{+/-}$ mice were setup for breeding to generate *Elane*$^{-/-}$ and littermate WT controls. *S*erum ALT, body weight, and liver weight were determined. (B) HFD-fed C57BL/6 mice were infected with Ad-*Cxcl1* and treated with an NET inhibitor Cl-amidine (50 mg/kg) at 7, 9, 11, and 13 days after Ad-*Cxcl1* infection. Serum levels of ALT, body weight, and liver weight on day 14 after Ad-*Cxcl1* infection are shown. (C) *Pad4*$^{Lyz-/-}$ and the littermate WT mice fed an HFD for 3 months followed by a 2-week infection with Ad-*Cxcl1* were sacrificed and subjected to analysis of serum ALT, body weight, and liver weight. Values represent mean ± SEM. Statistical evaluation was performed by Student's t-test.

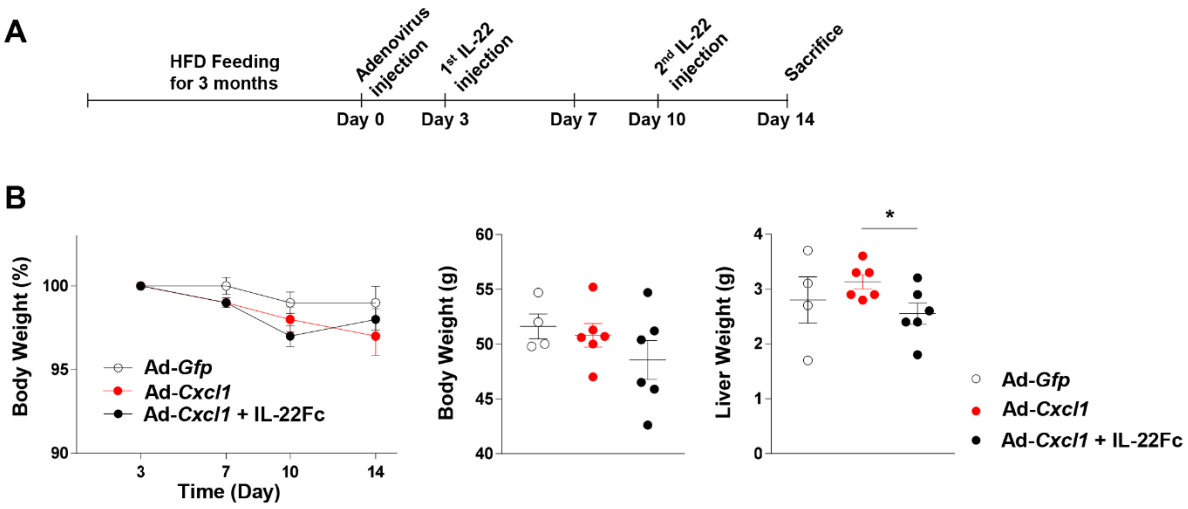

Supporting Fig. S7. IL-22Fc reduces liver weight but not body weight of mice. (A) A schematic illustration of the experimental design. (B) Changes in body weight during the treatment with IL-22Fc (left) and body weight and liver weight at sacrifice (right). Body weight at the moment of the 1st IL-22 administration was set at 100%. Values represent mean ± SEM. Statistical evaluation was performed by one-way ANOVA followed by Tukey's post hoc test for multiple comparisons (*p<0.05).

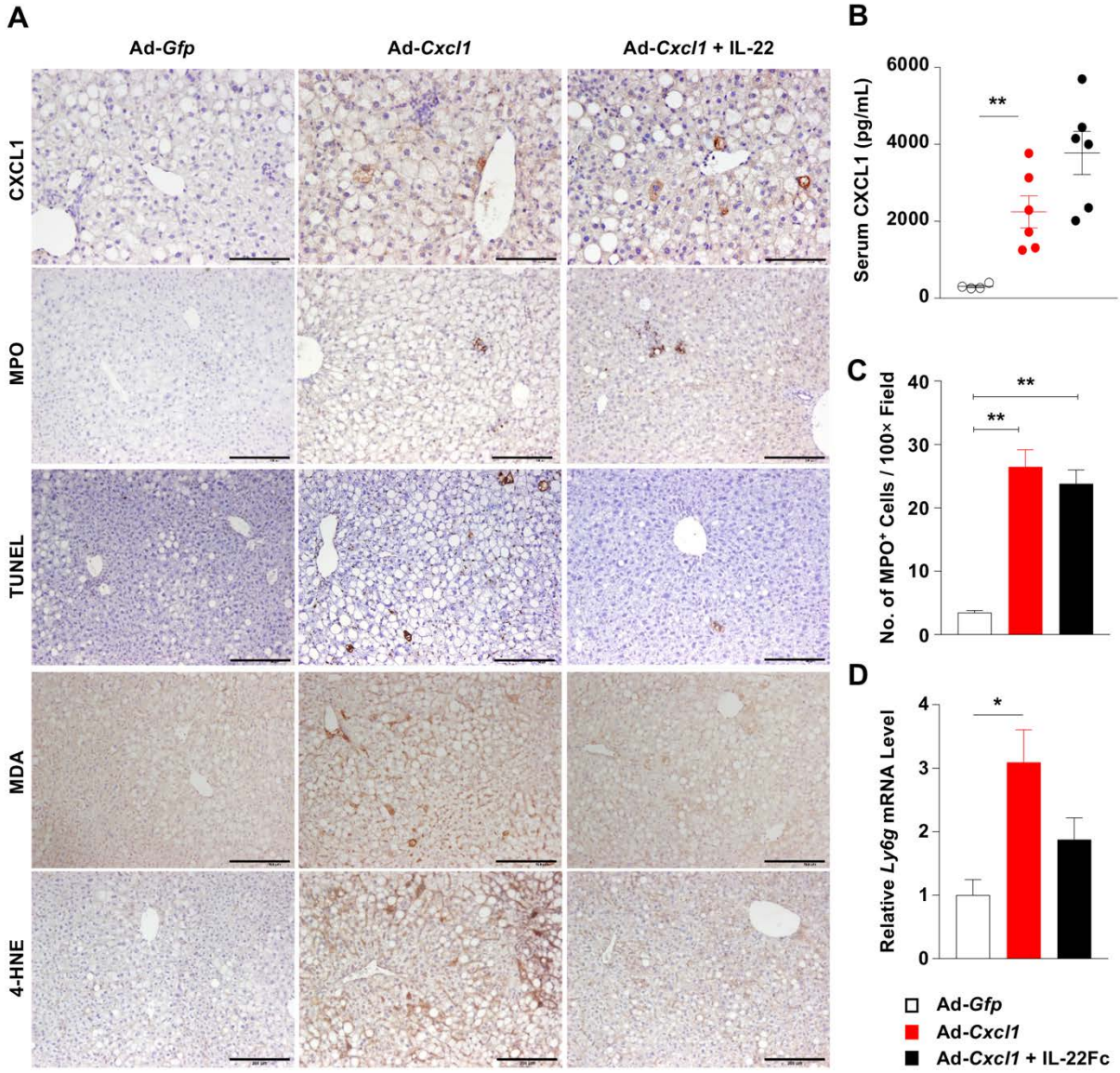

Supporting Fig. S8. IL-22Fc reduces liver injury and oxidative stress in CXCL1-induced NASH. (A) Paraffin-embedded liver sections of the mice which underwent the experimental procedure described in Supporting Fig. S7A were subjected to immunohistochemistry of CXCL1, MPO, TUNEL, MDA, and 4-HNE. Scale bars indicate 200 μm in every image except for CXCL1 (100 μm). (B) Serum levels of CXCL1 at sacrifice. (C) The number of MPO positive cells were determined from the images in panel (A). (D) RT-qPCR was performed to measure the hepatic mRNA levels of *Ly6g*, a neutrophil marker (n=4-6/group). Values represent mean ± SEM. Statistical evaluation was performed by one-way ANOVA followed by Tukey's post hoc test for multiple comparisons (*p<0.05, **p<0.01).

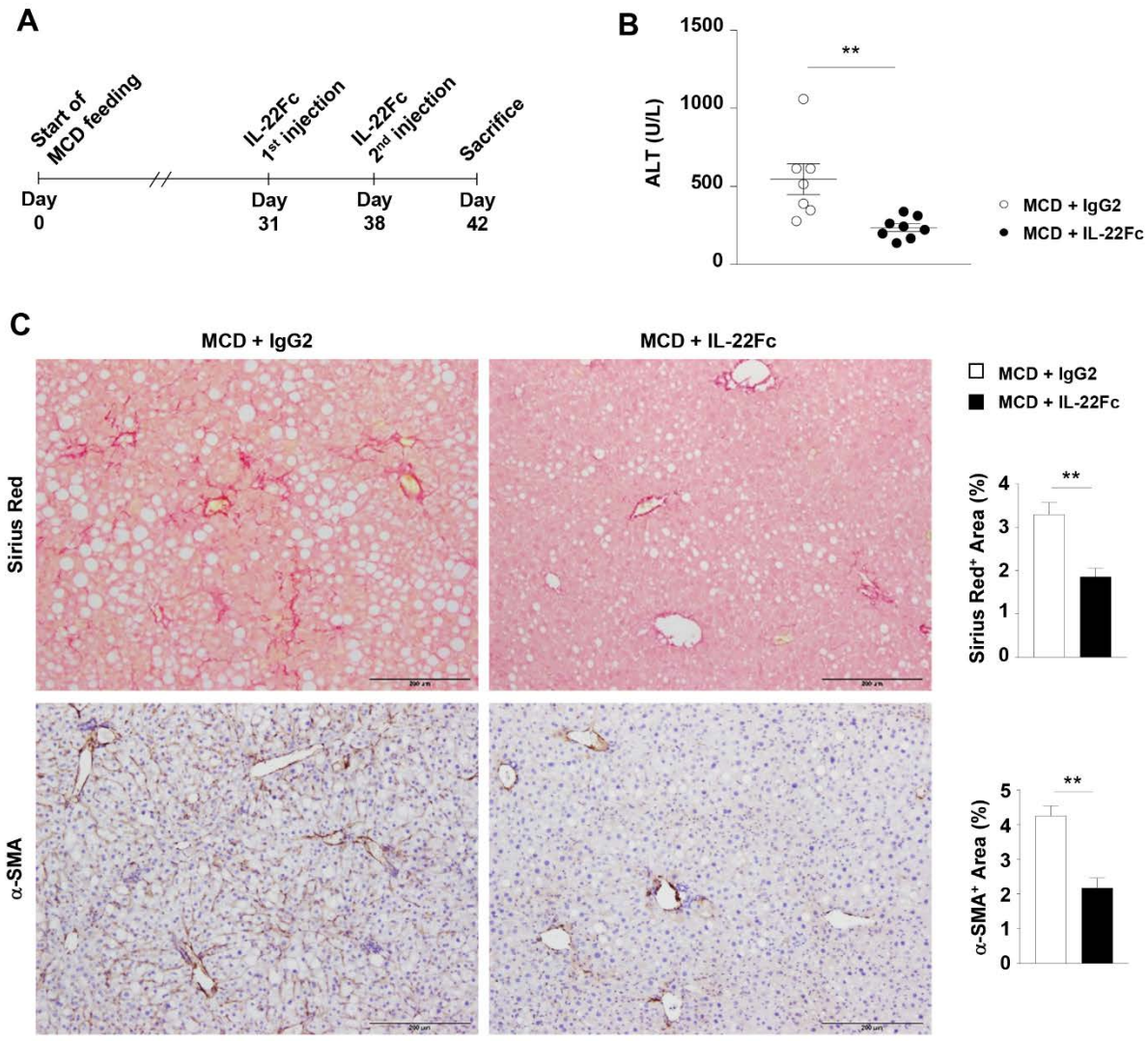

Supporting Fig. S9. IL-22Fc reduces liver injury and fibrosis in MCD-induced NASH. (A-C) Male C57BL/6J mice (n=7-8/group) were administered with IgG2 or IL-22Fc (0.5 mg/kg) on day 31 and day 38 after start of MCD feeding and were sacrificed on day 42 for analyses (panel A). Serum ALT levels (panel B). Histological analysis of Sirius Red and α-SMA in paraffin-embedded liver sections (left, panel C) and their quantification (right, panel C). Scale bars indicated 200 μm. Values represent mean ± SEM. Statistical evaluation was performed by Student's t-test (**p<0.01).

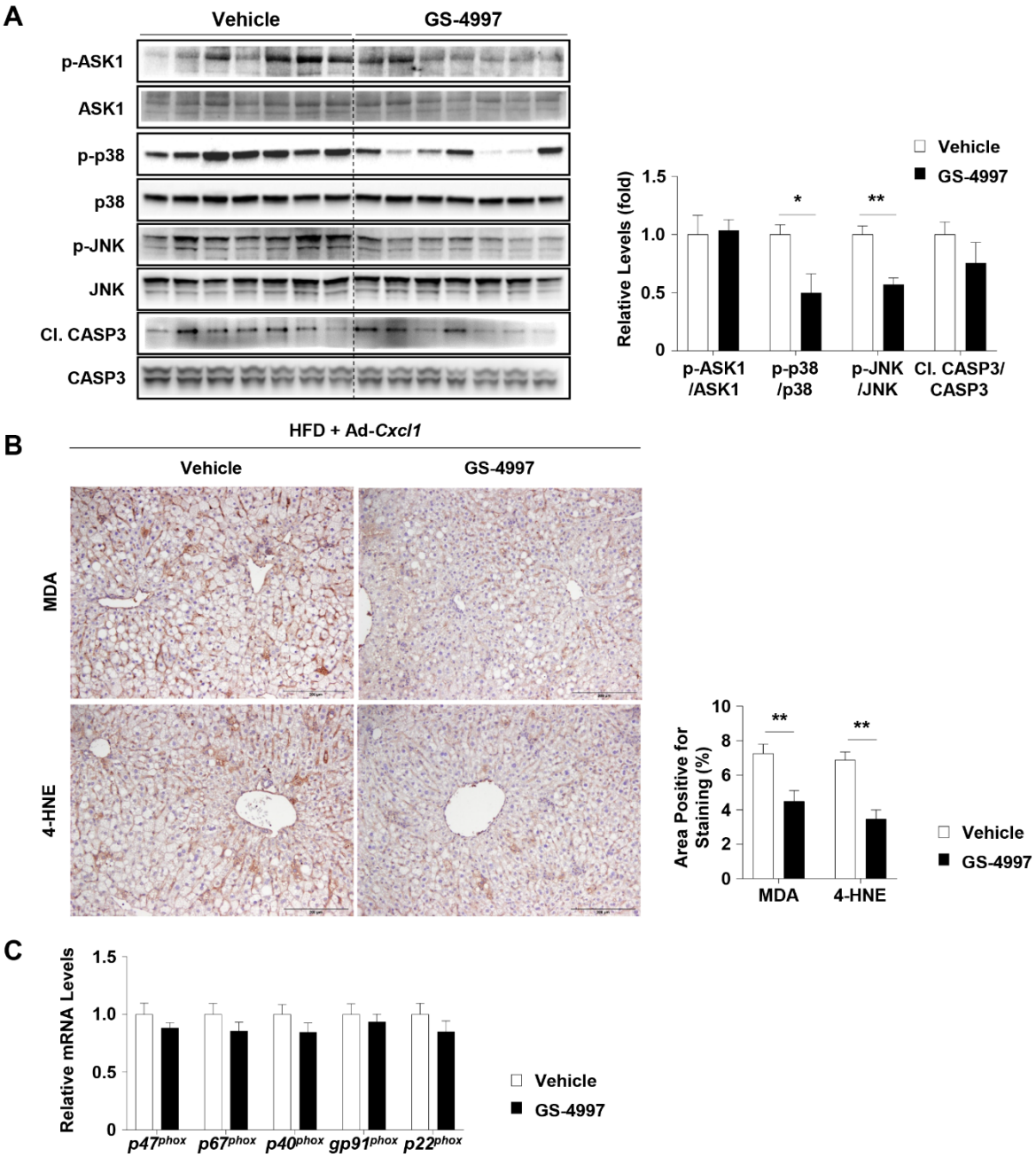

Supporting Fig. S10. GS-4997 reduces CXCL1-induced oxidative stress independently of NADPH oxidase 2 complex components. (A) C57BL/6J mice fed an HFD for 3 months were infected with Ad-*Cxcl1* and treated with GS-4997 (4 mg/kg) or vehicle. Hepatic expression of stress kinases and CASP3 was determined by immunoblot analysis (left) and the blots were quantified by densitometry (right). (B) Immunohistochemistry of MDA and 4-HNE in paraffin-embedded liver sections. Scale bars indicate 200 μm. (C) RT-qPCR was performed to measure the hepatic mRNA levels of NADPH oxidase 2 complex subunits (n=8/group). Values represent mean ± SEM. Statistical evaluation was performed by Student's t-test (*p<0.05, **p<0.01).

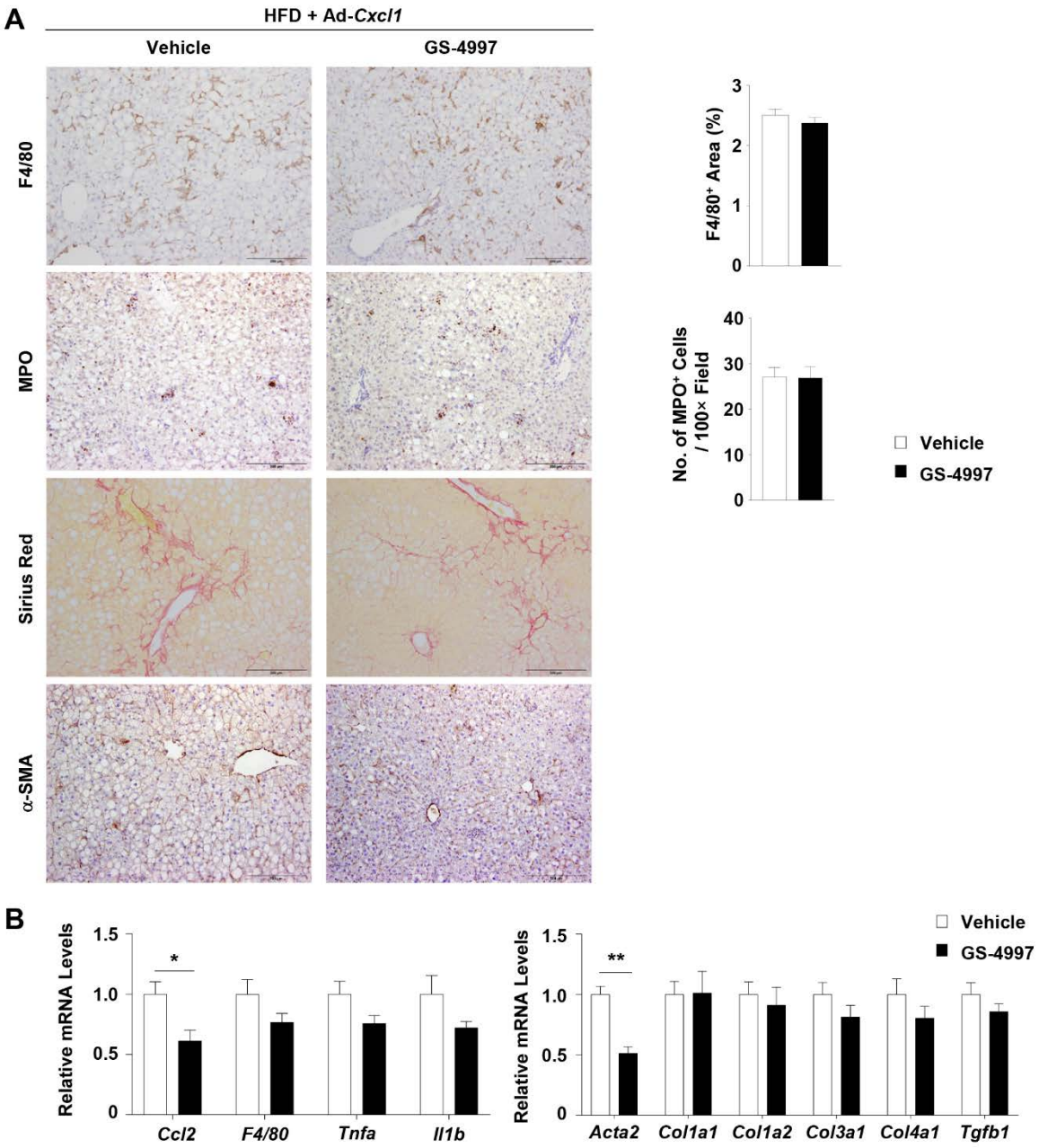

Supporting Fig. S11. GS-4997 fails to attenuate CXCL1-induced hepatic inflammation and fibrosis in HFD-fed mice. (A) Paraffin-embedded liver sections of HFD-fed, Ad-*Cxcl1*-infected C57BL/6J mice treated with GS-4997 (4 mg/kg) or vehicle were subjected to F4/80, MPO, Sirius Red, and α-SMA staining (left). Scale bars indicate 200 μm. Quantification of F4/80$^+$ area and the number of MPO$^+$ cells (right) (B) RT-qPCR was performed to measure the hepatic mRNA levels of inflammatory and fibrogenic genes (n=8/group). Values represent mean ± SEM. Statistical evaluation was performed by Student's t-test (*p<0.05, **p<0.01).

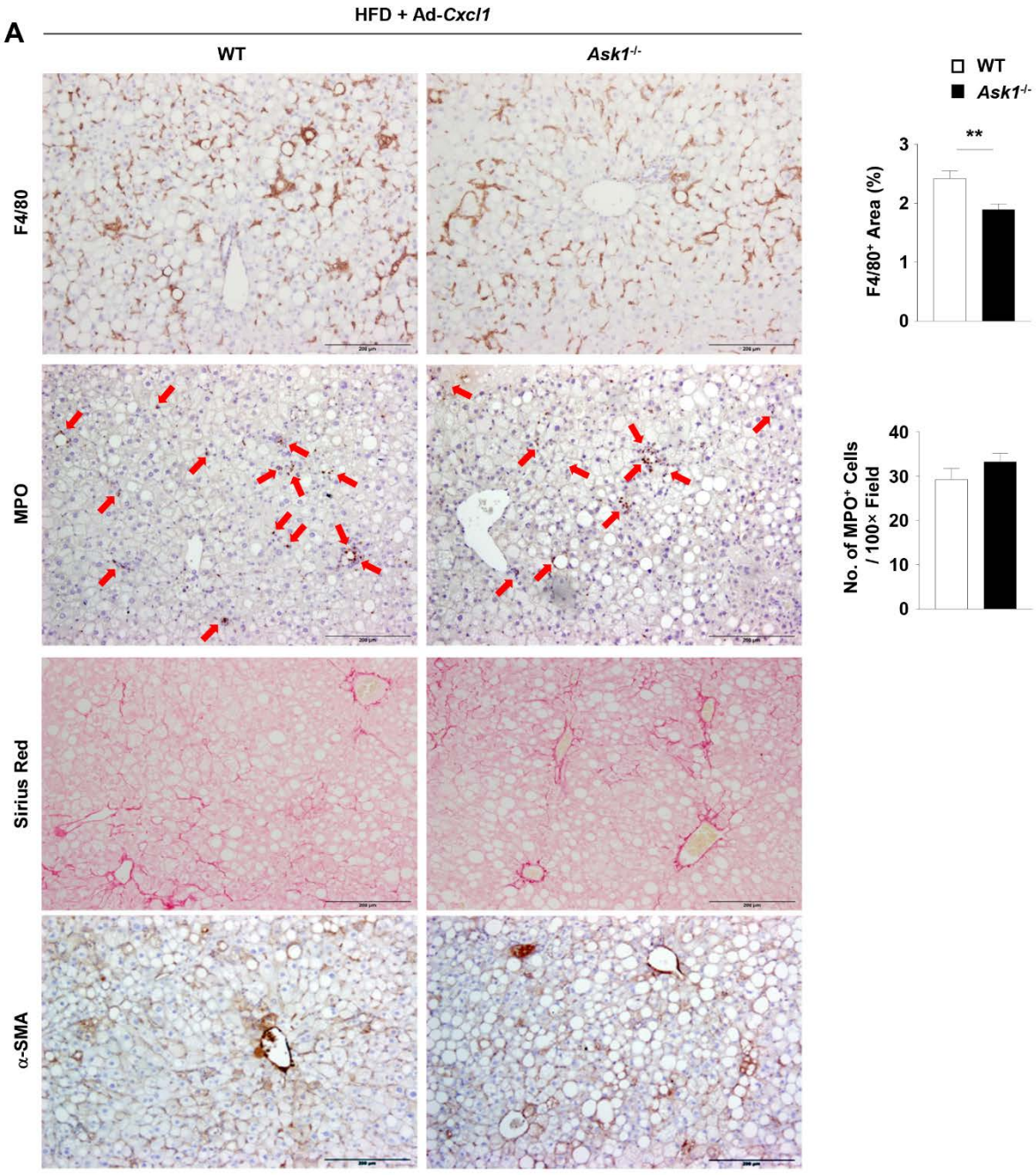

Supporting Fig. S12. Genetic ablation of *Ask1* attenuates CXCL1-induced hepatic inflammation but not fibrosis in HFD-fed mice. (A) Paraffin-embedded liver sections of *Ask1*$^{-/-}$ and the littermate WT mice were subjected to Sirius Red staining and immunohistochemistry of F4/80, MPO, and α-SMA. *Ask1*$^{+/-}$ mice were setup for breeding to generate *Ask1*$^{-/-}$ mice and their littermate WT mice. Red arrows indicate the clusters of MPO-positive cells. Scale bars indicate 200 μm. Values represent mean ± SEM. Statistical evaluation was performed by Student's t-test (**p<0.01).

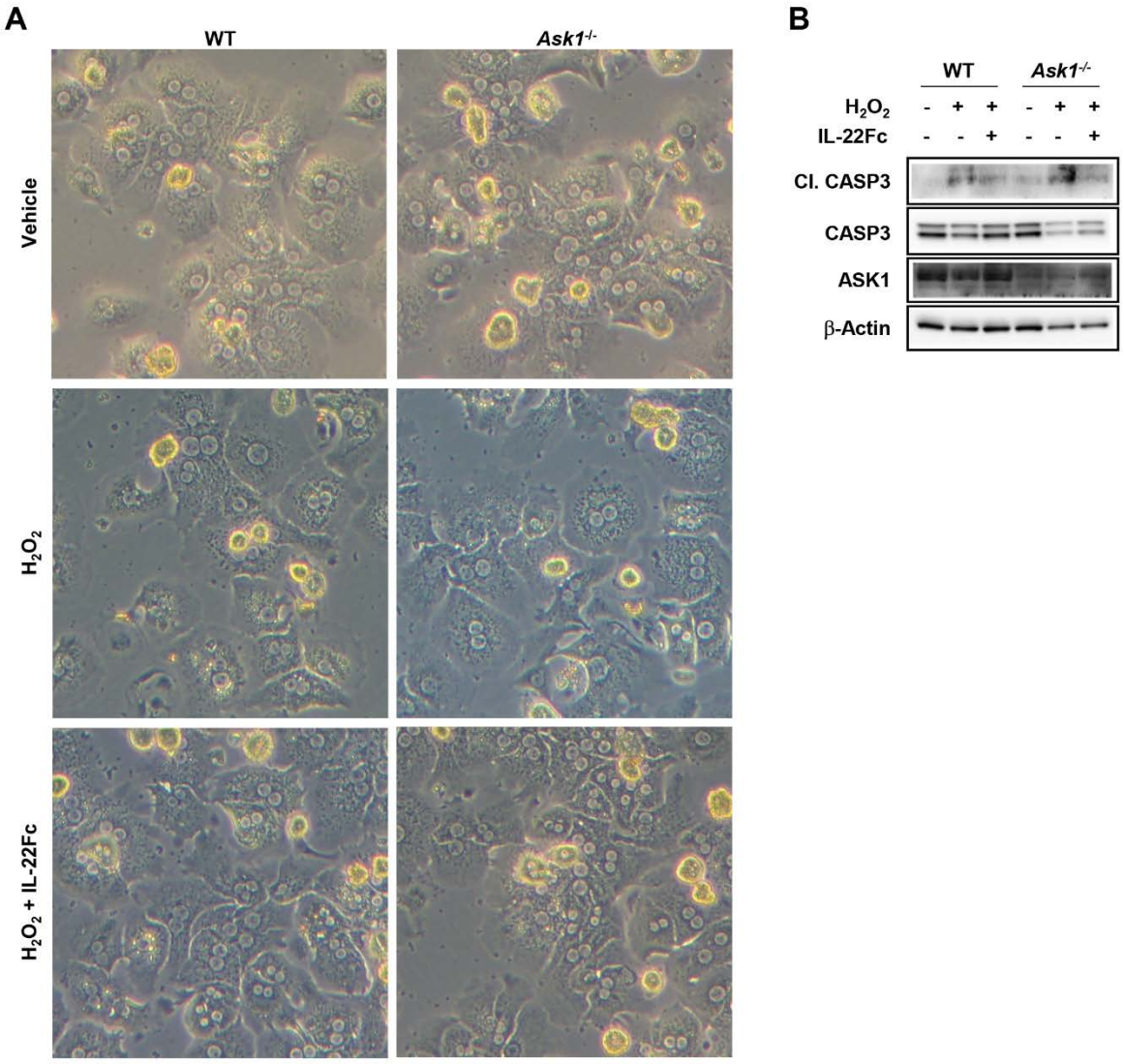

Supporting Fig. S13. The inhibitory effect of IL-22Fc on H_2O_2-induced hepatocyte death is independent of ASK1. (A) Primary WT and *Ask1*$^{-/-}$ hepatocytes were treated with H_2O_2 (0.5 mM) or vehicle for 5 hr preceded by a 18-hr pretreatment with IL-22Fc (50 ng/mL) or vehicle. Photomicrograph of cultured cells are shown (100X). (B) Cells from the same experimental conditions in panel (A) were lysed in RIPA buffer and subjected to immunoblot analysis.

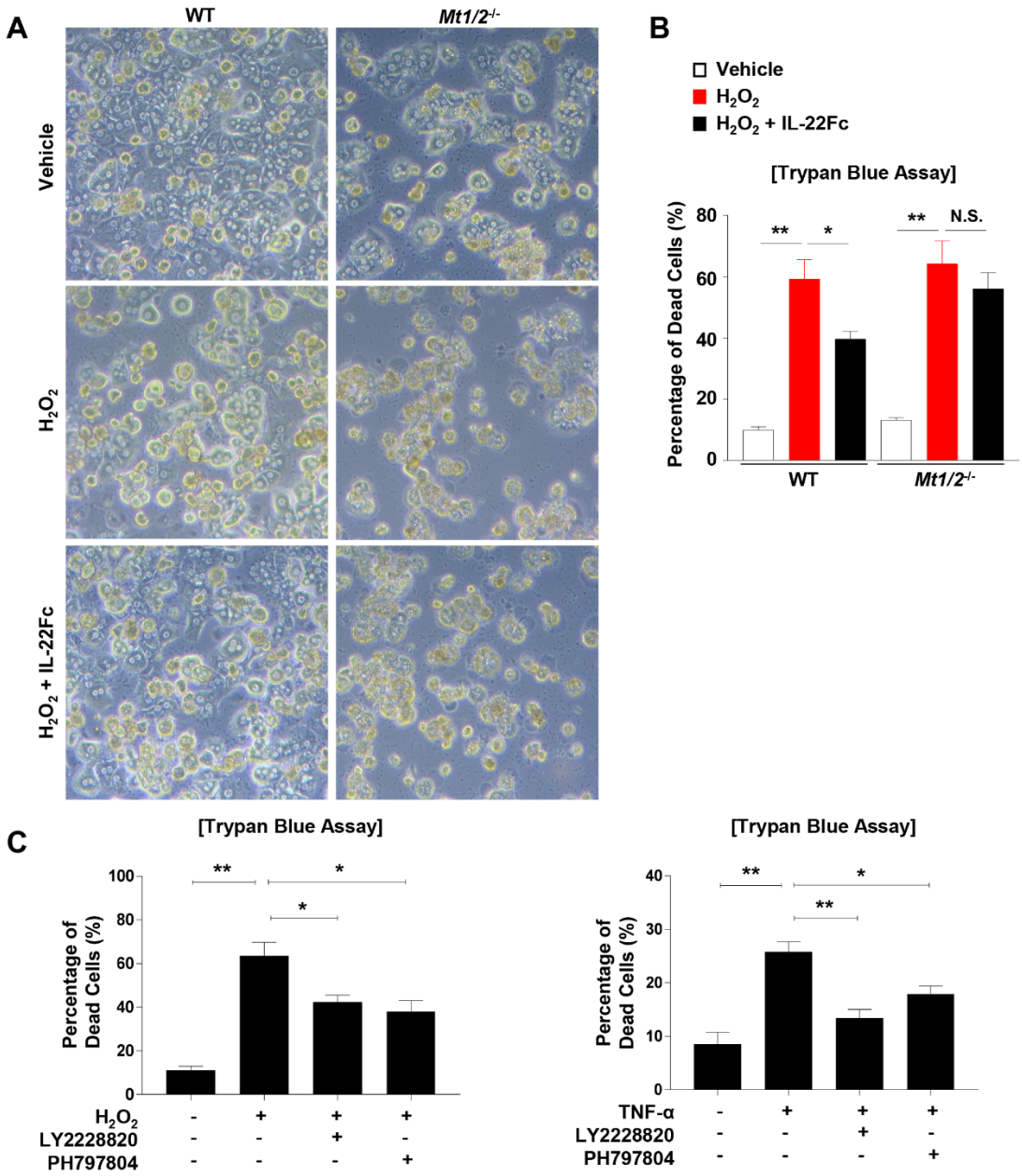

Supporting Fig. S14. The inhibitory effect of IL-22Fc on H_2O_2-induced hepatocyte death is dependent on MT, and p38 inhibition protects hepatocytes from H_2O_2- or TNF-α-induced death. (A) Primary *Mt1/2*$^{-/-}$ and WT hepatocytes were treated with H_2O_2 (0.5 mM) or vehicle for 5 hr preceded by a pretreatment with IL-22Fc (50 ng/mL) or vehicle for 18 hr. Photomicrograph of cultured cells are shown (100X). (B) Trypan blue assay was conducted to determine the percentage of dead cells from the same experimental conditions in panel (A) (n=3). (C) Mouse primary hepatocytes were treated with H_2O_2 (0.5 mM, 6 hr) or TNF-α (10 ng/mL, 24 hr) preceded by 1-hr pretreatment with the p38 inhibitor LY2228820 (1 μM) or PH797804 (5 μM). Trypan blue assay was conducted to determine the percentage of dead cells (n=3). Values represent mean ± SEM. Statistical evaluation was performed by one-way ANOVA followed by Tukey's post hoc test for multiple comparisons (*p<0.05; **p<0.01).

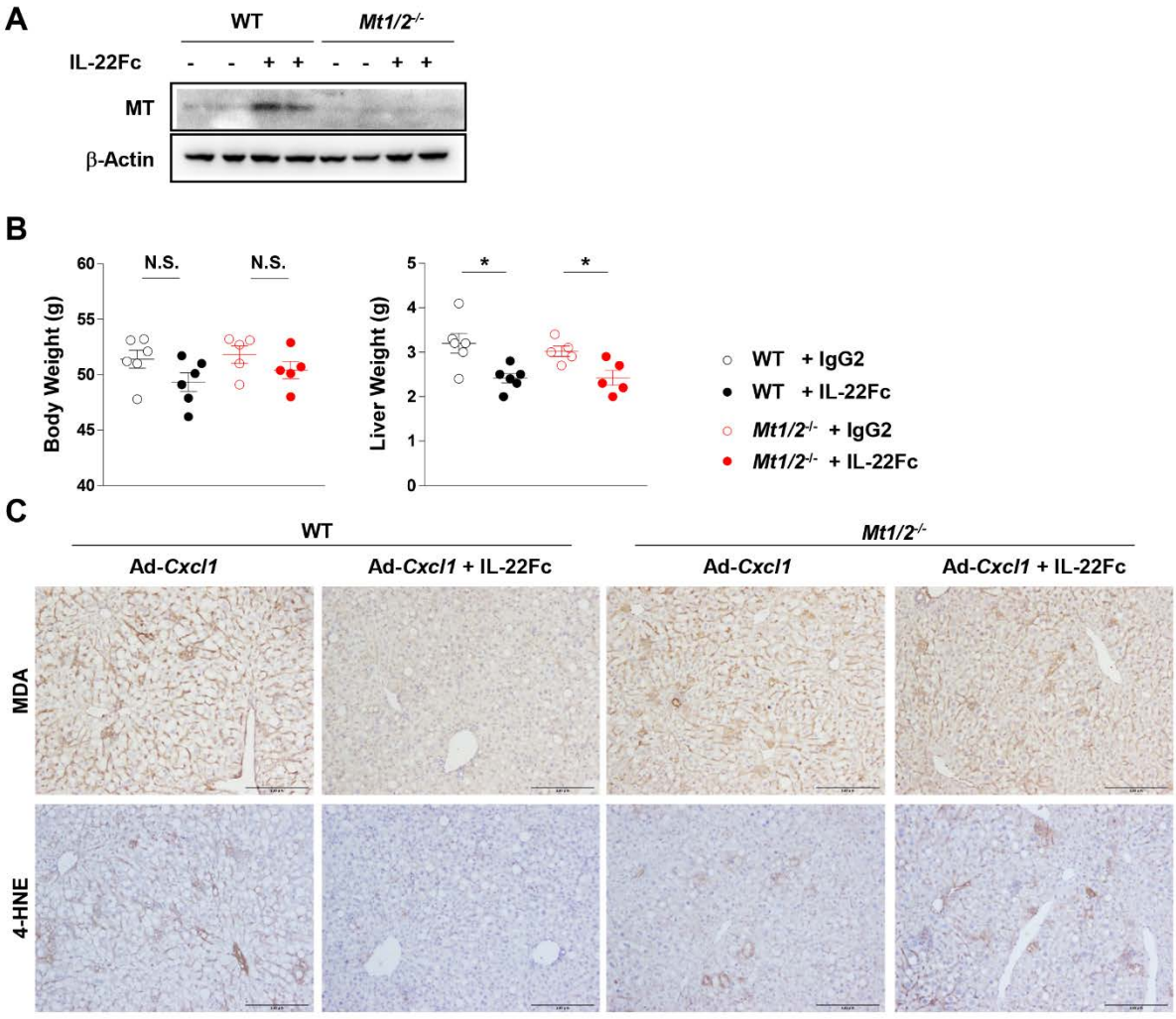

Supporting Fig. S15. MT contributes to the anti-oxidative functions of IL-22Fc in CXCL1-induced NASH. (A) *Mt1/2*$^{-/-}$ and the littermate WT control mice were treated with IL-22Fc (0.5 mg/kg) or IgG2 (n=5-6/group) in accordance with the experimental design illustrated in Supporting Fig. S7, and the liver homogenates were subjected to immunoblot analysis of MT. (B) Body weight and liver weight at sacrifice are shown. (C) Paraffin-embedded liver sections were subjected to immunohistochemistry of MDA and 4-HNE. Values represent mean ± SEM. Scale bars indicate 200 μm. Values represent mean ± SEM. Statistical evaluation was performed by one-way ANOVA followed by Tukey's post hoc test for multiple comparisons (*p<0.05).

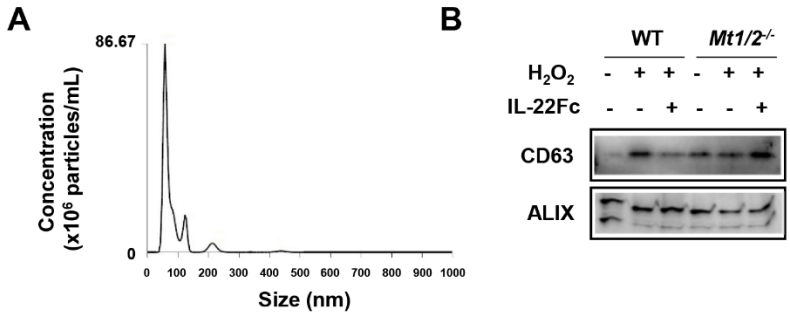

Supporting Fig. S16. Characterization of the hepatocyte-derived EVs. Hepatocyte-derived EVs were subjected to nanoparticle tracking analysis (A) and to immunoblot analysis of EV marker proteins (B).